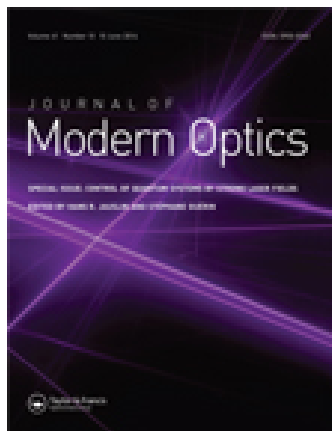


This article was downloaded by: [FU Berlin]

On: 13 August 2014, At: 11:38

Publisher: Taylor & Francis

Informa Ltd Registered in England and Wales Registered Number: 1072954 Registered office: Mortimer House, 37-41 Mortimer Street, London W1T 3JH, UK



Journal of Modern Optics

Publication details, including instructions for authors and subscription information:

<http://www.tandfonline.com/loi/tmop20>

Optimal control under spectral constraints: enforcing multi-photon absorption pathways

Daniel M. Reich^a, José P. Palao^b & Christiane P. Koch^a

^a Theoretische Physik, Universität Kassel, Heinrich-Plett-Str. 40, 34132 Kassel, Germany.

^b Departamento de Física Fundamental II and IUdEA, Universidad de La Laguna, Spain, La Laguna 38204, Spain.

Published online: 08 Nov 2013.



[Click for updates](#)

To cite this article: Daniel M. Reich, José P. Palao & Christiane P. Koch (2014) Optimal control under spectral constraints: enforcing multi-photon absorption pathways, *Journal of Modern Optics*, 61:10, 822-827, DOI: [10.1080/09500340.2013.844866](https://doi.org/10.1080/09500340.2013.844866)

To link to this article: <http://dx.doi.org/10.1080/09500340.2013.844866>

PLEASE SCROLL DOWN FOR ARTICLE

Taylor & Francis makes every effort to ensure the accuracy of all the information (the "Content") contained in the publications on our platform. However, Taylor & Francis, our agents, and our licensors make no representations or warranties whatsoever as to the accuracy, completeness, or suitability for any purpose of the Content. Any opinions and views expressed in this publication are the opinions and views of the authors, and are not the views of or endorsed by Taylor & Francis. The accuracy of the Content should not be relied upon and should be independently verified with primary sources of information. Taylor and Francis shall not be liable for any losses, actions, claims, proceedings, demands, costs, expenses, damages, and other liabilities whatsoever or howsoever caused arising directly or indirectly in connection with, in relation to or arising out of the use of the Content.

This article may be used for research, teaching, and private study purposes. Any substantial or systematic reproduction, redistribution, reselling, loan, sub-licensing, systematic supply, or distribution in any form to anyone is expressly forbidden. Terms & Conditions of access and use can be found at <http://www.tandfonline.com/page/terms-and-conditions>

Optimal control under spectral constraints: enforcing multi-photon absorption pathways

Daniel M. Reich^a, José P. Palao^b and Christiane P. Koch^{a*}

^aTheoretische Physik, Universität Kassel, Heinrich-Plett-Str. 40, 34132 Kassel, Germany; ^bDepartamento de Física Fundamental II and IUdEA, Universidad de La Laguna, Spain, La Laguna 38204, Spain

(Received 12 July 2013; accepted 10 September 2013)

Shaped pulses obtained by optimal control theory often possess unphysically broad spectra. In principle, the spectral width of a pulse can be restricted by an additional constraint in the optimization functional. However, it has so far been impossible to impose spectral constraints while strictly guaranteeing monotonic convergence. Here, we show that Krotov's method allows for simultaneously imposing temporal and spectral constraints without perturbing monotonic convergence, provided the constraints can be expressed as positive semi-definite quadratic forms. The optimized field is given by an integral equation which can be solved efficiently using the method of degenerate kernels. We demonstrate that Gaussian filters suppress undesired frequency components in the control of non-resonant two-photon absorption.

Keywords: optimal control theory; multi-photon absorption

1. Introduction

Optimal control theory (OCT) is a versatile mathematical tool to find external fields that drive the dynamics of a quantum system toward a desired outcome [1]. The controls are, e.g. the electric field of a laser pulse or the magnetic field amplitude of radio-frequency (RF) pulses. The underlying mechanism enabling the control are quantum interferences of light and matter [1,2]. OCT consists in formulating the physical target as a functional of the field which is then optimized. Typically, many solutions to the control problem exist [3], and it depends on additional constraints which of these solutions is found by an OCT algorithm. Such additional costs can be used to identify solutions that are feasible in control experiments, for example in feedback loops with shaped femtosecond laser pulses [4] or sequences of RF pulses in high-resolution nuclear magnetic resonance [5]. The constraints ensure, for example, a maximally allowed amplitude or smoothly switching the pulses on and off [6]. In principle, a constraint to ensure a given spectral width of the pulse can be formulated analogously [7]. It is highly desirable to include such a constraint since the spectral width is fixed in a given experiment. In order to compare theoretically calculated and experimentally obtained pulses, it is necessary to restrict the bandwidth of the calculated pulses to the experimental value. However, so far it has been impossible to impose spectral constraints while strictly guaranteeing monotonic convergence of the optimization algorithm. Without a spectral constraint, the optimized pulses often possess extremely broad spectra with

frequency components that are physically not necessary and cannot be realised experimentally, see, e.g. Ref. [7].

To obtain control over the frequency components of the optimal pulse, two alternatives to imposing spectral constraints as part of the optimization functional have recently been discussed. (i) The field can be expanded into frequency components, and the expansion coefficients, not the field itself, are optimized [8]. This approach requires a concurrent update of the field $\epsilon(t_i)$ for all t_i at once and cannot be combined with a sequential update. (ii) The optimized field can be filtered at the end of each iteration step to eliminate undesired frequency components [9–15]. The challenge consists in implementing the filtering in a way that does not destroy convergence of the algorithm. Formally, a filter can be obtained from a cost functional. However, the corresponding Lagrange multiplier which is decisive for the convergence of the algorithm, remains undetermined [10,13]. An educated guess for the Lagrange multiplier was shown to work under certain assumptions on the pulse and for sufficiently slow increase of the undesired frequency components [10,13]. It is nonetheless dissatisfying that monotonic convergence cannot be ensured in general. An alternative filtering approach that strictly enforces convergence interpolates between the unfiltered field obeying monotonic convergence and the completely filtered field destroying convergence. The strength of the filter is then chosen in such a way that the filter barely avoids breaking the convergence [11]. This approach comes with considerable extra numerical effort since the interpolation

*Corresponding author. Email: christiane.koch@uni-kassel.de

requires additional optimization runs for each value of the interpolation parameter.

Here, we demonstrate that spectral constraints can be included in the optimization functional without perturbing monotonic convergence using Krotov's method [16–19]. The spectral constraint is expressed via its Fourier transform as an integral over time. The corresponding integral kernel must be written as a positive semi-definite quadratic form. We show that this is the only requirement that needs to be met to ensure monotonic convergence. The modified update formula for the field corresponds to an inhomogeneous Fredholm equation of the second kind, i.e. an integral equation of the form $f(t) = g(t) + \lambda \int_a^b K(t, t') f(t') dt'$, where the inhomogeneity $g(t)$ and the kernel $K(t, t')$ are given and one seeks the solution $f(t)$. Such equations arise frequently in inversion problems and the theory of signal processing and can be solved efficiently using the method of degenerate kernels. Employing this approach, we apply Krotov's method including spectral constraints to the optimal control of non-resonant two-photon absorption.

2. Spectral constraints in Krotov's method

In optimal control theory, the optimization problem is formulated by stating the target and additional constraints in functional form,

$$J[\{\psi_k\}, \epsilon] = J_T[\{\psi_k(T)\}] + J_a[\epsilon] + J_b[\{\psi_k\}], \quad (1)$$

where J_T denotes the target at final time T and $\{\psi_k(t)\}$ is a set of state vectors describing the time evolution of the system. $\epsilon(t)$ is a real function representing the control variable, e.g. the electric field amplitude of a laser pulse. All additional constraints are assumed to depend either on the control or on the states,

$$J_a = \int_0^T g_a(\epsilon, t) dt, \quad J_b = \int_0^T g_b(\{\psi_k\}, t) dt. \quad (2)$$

A common choice for $g_a(\epsilon, t)$ minimizes the pulse intensity or change in pulse intensity [18],

$$g_a(\epsilon, t) = \frac{\lambda_0}{S(t)} [\epsilon(t) - \epsilon^{(0)}(t)]^2 = \frac{\lambda_0}{S(t)} [\Delta\epsilon(t)]^2, \quad (3)$$

with λ_0 a weight to favor solutions with lower pulse amplitude and $S(t)$ a shape function to smoothly switch the pulse on and off. J_b can be used to restrict the time evolution to a subspace of the Hilbert space or to optimize a time-dependent target, see Ref. [19] and references therein.

Minimization of the functional (1) yields a set of coupled equations for the states and the control. The non-linear optimization method developed by Konnov and Krotov [16] provides a general, monotonically convergent algorithm. Given Equation (3) for g_a , it updates the control at iteration step $i + 1$ according to [19]

$$\begin{aligned} \epsilon^{(i+1)}(t) = \epsilon^{(i)}(t) + \frac{S(t)}{\lambda_0} \Im \left\{ \sum_k \left\langle \chi_k^{(i)}(t) \left| \frac{\partial \hat{\mathbf{H}}}{\partial \epsilon} \right| \psi_k^{(i+1)}(t) \right\rangle \right. \\ \left. + \frac{1}{2} \sigma(t) \sum_k \left\langle \Delta \psi_k(t) \left| \frac{\partial \hat{\mathbf{H}}}{\partial \epsilon} \right| \psi_k^{(i+1)}(t) \right\rangle \right\}, \quad (4) \end{aligned}$$

where $|\Delta \psi_k(t)\rangle = |\psi_k^{(i+1)}(t)\rangle - |\psi_k^{(i)}(t)\rangle$ and $\hat{\mathbf{H}}$ is the Hamiltonian of the system. The adjoint states $|\chi_k(t)\rangle$ are propagated backwards in time with the boundary condition $|\chi_k(T)\rangle$ determined by the final-time target J_T . The choice of the function $\sigma(t)$ allows for ensuring monotonic convergence [16]. The specific form of $\sigma(t)$ depends on the optimization functional and the equations of motion. It can be estimated analytically or determined numerically, based on the optimization history [19].

Constraints on the spectrum of the control have to be included in the cost functional J_a . Monotonic convergence requires a well-defined sign of J_a [18,19]. A general expression that fulfills this requirement is obtained by writing J_a as a quadratic form. In the frequency domain, necessary to formulate spectral constraints, the cost functional thus becomes

$$\begin{aligned} J_a(\epsilon) &= \int_{-\infty}^{\infty} \Delta\epsilon(\omega) \bar{K}(\omega) \Delta\epsilon^*(\omega) d\omega \\ &= \frac{1}{2\pi} \int_{-\infty}^{\infty} \int_{-\infty}^{\infty} \Delta\epsilon(t) K(t-t') \Delta\epsilon(t') dt' dt, \end{aligned}$$

where a real kernel function \bar{K} in the frequency domain and its Fourier transform K in the time domain have been introduced. The desired spectral constraints are thus implemented by the kernel function. Given Equation (5) for J_a , the function g_a , defined in Equation (2), takes the form

$$g_a(\epsilon, t) = \frac{1}{2\pi} \int_0^T \Delta\epsilon(t) K(t-t') \Delta\epsilon(t') dt'. \quad (5)$$

Since the field and thus the change in the field are zero outside of the interval $[0, T]$, integration can be restricted to $[0, T]$. In Krotov's method, monotonic convergence can be ensured if the kernel $K(t-t')$ is positive semi-definite [19]. This follows directly from the condition for the change of the functional due to changes in the control to be positive [18,19] which in turn translates into g_a being a convex function. Equivalently in the frequency domain, $\bar{K}(\omega)$ has to be positive semi-definite. Monotonic convergence is therefore guaranteed if

$$\bar{K}(\omega) \geq 0 \quad \forall \omega. \quad (6)$$

Since derivation of the update equation requires evaluation of $\partial g_a / \partial \epsilon$ as a function of time [17–19], the Fourier transform of $\bar{K}(\omega)$ should have a closed form in addition to being positive semi-definite. For numerical stability, it is furthermore desirable to use smooth kernels. A suitable choice fulfilling these requirements are Gaussian kernels,

$$\begin{aligned}\bar{K}(\omega) &= \lambda_a - \sum_i \frac{\lambda_b^i}{2} \left[\exp\left(-\frac{(\omega - \omega_i)^2}{2\sigma_i^2}\right) \right. \\ &\quad \left. + \exp\left(-\frac{(\omega + \omega_i)^2}{2\sigma_i^2}\right) \right], \\ K(t - t') &= 2\pi\lambda_a\delta(t - t') - \sum_i \lambda_b^i (2\pi\sigma_i^2)^{1/2} \\ &\quad \times \cos[\omega_i(t - t')] \exp\left(-\frac{\sigma_i^2(t - t')^2}{2}\right).\end{aligned}\quad (7)$$

Note that we choose symmetric Gaussian kernels since we consider here real fields. An extension to complex controls is straightforward. For (approximately) non-overlapping Gaussians in the frequency domain, monotonic convergence is obtained if

$$\lambda_b^i \leq 2\lambda_a \quad \forall i. \quad (8)$$

The first term in Equation (7) reproduces Equation (3) with $\lambda_0 = \lambda_a$ and $S(t) = 1$. For $\lambda_b^i > 0$, the kernel (7) implements a frequency pass for $\Delta\epsilon(t)$ around the frequencies ω_i . For $\lambda_b^i < 0$, a frequency filter for $\Delta\epsilon(t)$ around the frequencies ω_i is obtained. Due to the condition (8), frequency passes are not guaranteed to be effective, i.e. the λ_b^i might be too small for the spectral constraint to gain sufficient weight. For frequency filters, no such restriction exists. A work-around to create effective frequency passes consists therefore in adding up sufficiently many frequency filters. Moreover, an amplitude constraint with non-constant shape function can be reintroduced additively in the time domain for $\lambda_b^i < 0$, setting $\lambda_a = 0$. This does not perturb monotonic convergence since both amplitude and frequency constraint preserve monotonic convergence individually.

Following the prescription of Ref. [19], the update equation for Gaussian band filters around frequencies ω_i and an additional amplitude constraint imposed by a shape function $\lambda_0/S(t)$ is obtained as

$$\begin{aligned}\epsilon^{(i+1)}(t) &= \epsilon^{(i)}(t) + \sum_i \frac{\lambda_b^i S(t)}{2\pi\lambda_0} (2\pi\sigma_i^2)^{1/2} \\ &\quad \times \int_0^T \cos[\omega_i(t - t')] \exp\left(-\frac{\sigma_i^2(t - t')^2}{2}\right) \\ &\quad \times \left(\epsilon^{(i+1)}(t') - \epsilon^{(i)}(t') \right) dt' + \frac{S(t)}{\lambda_0} \\ &\quad \times \Im \left\{ \sum_k \left\langle \chi_k^{(i)}(t) \left| \frac{\partial \hat{\mathbf{H}}}{\partial \epsilon} \right| \psi_k^{(i+1)}(t) \right\rangle \right. \\ &\quad \left. + \frac{1}{2} \sigma(t) \sum_k \left\langle \Delta \psi_k(t) \left| \frac{\partial \hat{\mathbf{H}}}{\partial \epsilon} \right| \psi_k^{(i+1)}(t) \right\rangle \right\}.\end{aligned}\quad (9)$$

This is an implicit equation for $\epsilon^{(i+1)}(t)$. It is possible to rewrite Equation (9) as a Fredholm integral equation of the

second kind for $\Delta\epsilon(t) = \epsilon^{(i+1)}(t) - \epsilon^{(i)}(t)$,

$$\Delta\epsilon(t) = I(t) + \gamma \int_0^T \mathcal{K}(t, t') \Delta\epsilon(t') dt'. \quad (10)$$

The inhomogeneity $I(t)$ depends on the unknown states $\{\psi_k^{(i+1)}(t)\}$. They can be approximated by calculating $\Delta\epsilon(t)$ according to Equation (4), i.e. without frequency constraints. Propagating the states under that field yields an approximation of $I(t)$. In our applications this turned out to be sufficient. However, if the quality of the resulting approximation of $I(t)$ is not good enough, the field obtained from a first solution of the Fredholm equation can be used to propagate the states and obtain an improved approximation of $I(t)$. This procedure can be repeated iteratively until the desired accuracy is reached. The remaining question is then how to solve the integral equation (10).

Often, Fredholm equations of the second kind are solved numerically [20] by quadrature of the integral,

$$\int_0^T \mathcal{K}(t, t') \Delta\epsilon(t') dt' \simeq \sum_{j=1}^N w_j \mathcal{K}(t, t_j) \Delta\epsilon(t_j)$$

such that

$$\Delta\epsilon(t_k) \simeq I(t_k) + \gamma \sum_{j=1}^N w_j \mathcal{K}(t_k, t_j) \Delta\epsilon(t_j),$$

or collocation, i.e. expanding $\Delta\epsilon(t)$ into orthonormal basis functions $c_j(t)$ on $[0, T]$,

$$\Delta\epsilon(t) = \sum_{j=1}^N a_j c_j(t).$$

In both cases, solution of the integral equation is reduced to solving a system of linear equations. Alternatively, a Fredholm equation of the second kind can be solved by approximating $\mathcal{K}(t, t')$ by a degenerate kernel, $\mathcal{K}_N(t, t') = \sum_{j=1}^N \alpha_j(t) \delta_j(t')$ [20]. Solution of a Fredholm degenerate integral equation again reduces to solving a system of linear equations. For our purposes, an approach based on degenerate kernels [21,22] turns out to be the best option. It is more stable than collocation and similar to the quadrature of the integral but more direct since the kernel rather than the integral is approximated. The solution to Equation (10) is then given by

$$\Delta\epsilon(t) = I(t) + \sum_{j=0}^N X_j \alpha_j(t) \quad (11)$$

with $\alpha_j(t)$ defined in Equation (12) and X_j the solution of the system of linear equations (13).

3. Control of non-resonant two-photon absorption

We apply Krotov's method including spectral constraints, Equation (9), to non-resonant two-photon absorption in

sodium atoms. The goal is to transfer population from level $|3s\rangle$ to $|4s\rangle$. Due to selection rules, this is possible only by absorption of two photons with the transition dipoles provided by the off-resonant $|np\rangle$ levels with the main contribution coming from $|3p\rangle$. We do not invoke an adiabatic elimination of all off-resonant levels, i.e. our Hamiltonian includes $\{|3s\rangle, |4s\rangle, |np\rangle\}$ with $n = 3, \dots, 8$ and the corresponding $s - p$ transition dipole moments, taken from Ref. [23]. Our example thus corresponds to the standard quantum control problem of population transfer, Schrödinger dynamics and linear light–matter coupling which can be solved by the first-order variant of Krotov’s method [19], i.e. $\sigma(t) = 0$ in Equations (4) and (9). Within this model, two control strategies are available to transfer population from $|3s\rangle$ to $|4s\rangle$ – resonant two-color one-photon transitions with frequencies $\omega_{3s,3p}$ and $\omega_{3p,4s}$ or an off-resonant two-photon transition with frequency close to $\omega_{3s,4s}/2$.

Non-resonant two-photon absorption has been studied experimentally for ns to $(n + 1)s$ transitions in alkali atoms in the weak [24–26], strong [27–29] and intermediate field regime [30–33]. To date, optimal control calculations of non-resonant two-photon absorption have been hampered by a spectral spread of the field. The resulting spectral widths by far exceed experimentally realistic values. As a result, only solutions using one-photon transitions are found while the experimental result of *non-resonant* two-photon control [24–33] could not be reproduced. Here we employ optimal control theory with spectral constraints to enforce a non-resonant two-photon solution. We use Gaussian frequency filters around the one-photon transition frequencies to suppress resonant dipole transitions.

Figure 1 compares the optimal pulses and their spectra obtained by Krotov’s method with (bottom panel) and without (top panel) spectral constraint, cf. Equations (9) and (4). The frequency filters around the one-photon transition frequencies are indicated in red in Figure 1(d). The central frequency of the guess pulse is taken to be exactly the two-photon transition frequency. Its peak amplitude is about a fourth of that of a two-photon π -pulse. Despite the guess pulse being fairly close to a non-resonant two-photon solution, the optimization algorithm yields a pulse that uses the resonant one-photon transitions, cf. the three small peaks in Figure 1(b). This is rationalized in terms of the intensity which should increase as little as possible according to the constraint (3) and resonant transitions requiring a lot less intensity than non-resonant ones. Increasing the spectral width comes at no ‘cost’ for the optimization algorithm when no spectral constraint is present. Thus solutions that use resonant one-photon transitions and have a broad spectral width are the natural ones for optimization without spectral constraint. Once the spectral constraint is included, the optimization algorithm increases the pulse amplitude until a two-photon Rabi frequency of π is hit. The spectrum of the optimal pulse is hardly modified compared to that of the guess pulse.

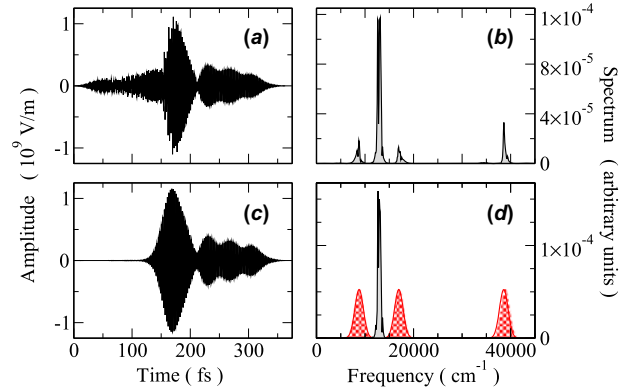


Figure 1. Optimized pulses and their spectra with ((c)+(d)) and without ((a)+(b)) spectral constraint. The Gaussian filters employed in the spectral constraint are shown in red. (The color version of this figure is included in the online version of the journal.)

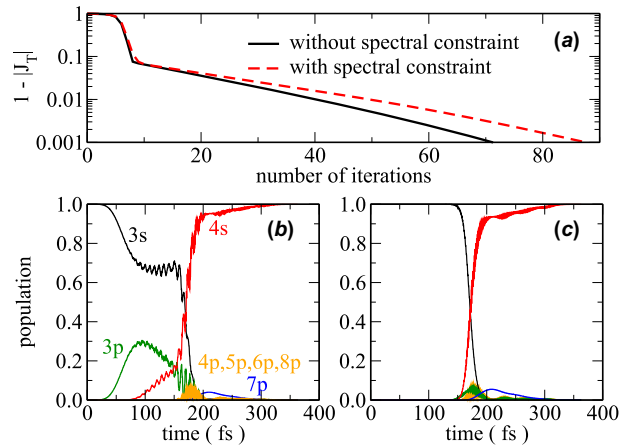


Figure 2. Convergence toward the optimum (a) and dynamics under the optimized pulses with (c) and without (b) spectral constraint. (The color version of this figure is included in the online version of the journal.)

Imposing an additional constraint results in a more difficult optimization problem. This is illustrated by Figure 2(a) which compares the convergence toward the optimum for optimization with and without the spectral constraint. In order to reach the optimum within an ‘error’, $\varepsilon = 1 - |J_T|$, of 10^{-3} the number of iterations is increased from 71 to 87. The slower convergence of the algorithm with spectral constraint is attributed to optimization under two conflicting costs – keeping the intensity as low as possible while avoiding certain spectral regions. The algorithm needs to balance the two conflicting costs, which results in a more difficult optimization problem.

While the increase in the number of iterations, when adding the spectral constraint, is comparatively moderate, a CPU time of about 370 s is needed for 10 iterations, compared to only 6 s for the algorithm without spectral constraint. This is due to the additional numerical effort required in order to solve the Fredholm equation. This effort

scales with the number of time grid points but is independent of the complexity of the system. The comparison of the CPU time required with and without the spectral constraint will be much more favorable for more complex systems. Then most of the CPU time will be spent for the time propagation whereas the solution of the Fredholm equation represents a comparatively small add-on. Moreover, the numerical effort for solving the Fredholm equation can be further reduced by exploiting the bandedness of the matrix in Equation (13).

4. Summary

We have derived an extension of Krotov's method for quantum optimal control that allows for including constraints on the control in the frequency and the time domain at the same time. The key is to ensure a well-defined sign of the integral over the spectral constraint which we have achieved by expressing the constraint as a quadratic form. Kernels consisting of sums over Gaussians, to be used either as frequency passes or as frequency filters, turn out to be the most practical choice. Since the Fourier transform of such a frequency constraint is known analytically, a closed form of the update equation is obtained. Monotonicity of the algorithm imposes a limit on the weight of the constraint for frequency passes. Therefore frequency passes may be inefficient. On the other hand, frequency filters can be employed without restriction. A practical work-around for frequency passes thus consists in summing up sufficiently many frequency filters.

The update equation that we obtain for Gaussian frequency filters is an implicit equation in the control which takes the form of a Fredholm integral equation of the second kind. It can be solved accurately and efficiently using the method of degenerate kernels [21,22]. Our results for non-resonant two-photon absorption in sodium atoms show an excellent restriction on the spectrum of the optimized pulse. The new algorithm thus allows for reproducing experimentally known control strategies for strong-field non-resonant two-photon absorption [27–29]. It can also be used in conjunction with quasi-Newton methods in order to achieve faster convergence [34]. In future work, we will discuss in detail how the spectral constraint allows for steering the optimization pathway in the control landscape [35].

Acknowledgements

We would like to thank Ronnie Kosloff for many valuable discussions.

Funding

Financial support from the Deutsche Forschungsgemeinschaft (grant No. KO 2301/2) and by the Spanish MICINN (grant No. FIS2010-19998) is gratefully acknowledged.

References

- [1] Rice, S.A.; Zhao, M. *Optical Control of Molecular Dynamics*; Wiley, New York, **2000**.
- [2] Brumer, P.; Shapiro, M. *Principles and Applications of the Quantum Control of Molecular Processes*; Wiley VCH, Weinheim, **2011**.
- [3] Rabitz, H.A.; Hsieh, M.M.; Rosenthal, C.M. *Science* **2004**, *303*, 1998–2001.
- [4] Rabitz, H.; de Vivie-Riedle, R.; Motzkus, M.; Kompa, K. *Science* **2000**, *288*, 824–828.
- [5] Skinner, T.E.; Reiss, T.O.; Luy, B.; Khaneja, N.; Glaser, S.J. *J. Magn. Reson.* **2003**, *163*, 8–15.
- [6] Sundermann, K.; de Vivie-Riedle, R. *J. Chem. Phys.* **1999**, *110* (4), 1896–1904.
- [7] Koch, C.P.; Palao, J.P.; Kosloff, R.; Masnou-Seeuws, F. *Phys. Rev. A* **2004**, *70*, 013402.
- [8] Skinner, T.E.; Gershenson, N.I. *J. Magn. Reson.* **2010**, *204*, 248–255.
- [9] Werschnik, J.; Gross, E. *J. Opt. B: Quantum Semiclassical Opt.* **2005**, *7*, S300.
- [10] Gollub, C.; Kowalewski, M.; de Vivie-Riedle, R. *Phys. Rev. Lett.* **2008**, *101*, 073002.
- [11] Lapert, M.; Tehini, R.; Turinici, G.; Sugny, D. *Phys. Rev. A* **2009**, *79*, 063411.
- [12] Schröder, M.; Brown, A. *New J. Phys.* **2009**, *11*, 105031.
- [13] Gollub, C.; Kowalewski, M.; Thallmair, S.; de Vivie-Riedle, R. *Phys. Chem. Chem. Phys.* **2010**, *12*, 15780–15787.
- [14] Motzoi, F.; Gambetta, J.M.; Merkel, S.T.; Wilhelm, F.K. *Phys. Rev. A* **2011**, *84*, 022307.
- [15] Schaefer, I.; Kosloff, R. *Phys. Rev. A* **2012**, *86*, 063417.
- [16] Konnov, A.; Krotov, V. *Autom. Remote Control* **1999**, *60*, 1427–1436.
- [17] Sklarz, S.E.; Tannor, D. *J. Phys. Rev. A* **2002**, *66*, 053619.
- [18] Palao, J.P.; Kosloff, R. *Phys. Rev. A* **2003**, *68*, 062308.
- [19] Reich, D.M.; Ndong, M.; Koch, C.P. *J. Chem. Phys.* **2012**, *136*, 104103.
- [20] *Encyclopedia of Mathematics*, Springer The European Mathematical Society; <http://www.encyclopediaofmath.org/> (accessed Jun 12, 2013).
- [21] Volk, W. *Die numerische Behandlung Fredholm'scher Integralgleichungen zweiter Art mittels Splinefunktionen*; Report HMI-B286; Hahn-Meitner-Institut für Kernforschung, Berlin, 1979.
- [22] Volk, W.J. *Integral Equations* **1985**, *9*, 171–190.
- [23] Kramida, A.; Ralchenko, Y.; Reader, J.; NIST ASD Team. *NIST Atomic Spectra Database (version 5.0)*. <http://physics.nist.gov/asd> (accessed Jun 12, 2013).
- [24] Meshulach, D.; Silberberg, Y. *Nature* **1998**, *396*, 239–242.
- [25] Meshulach, D.; Silberberg, Y. *Phys. Rev. A* **1999**, *60*, 1287–1292.
- [26] Präkelt, A.; Wollenhaupt, M.; Sarpe-Tudoran, C.; Baumert, T. *Phys. Rev. A* **2004**, *70*, 063407.
- [27] Trallero-Herrero, C.; Cardoza, D.; Weinacht, T.C.; Cohen, J.L. *Phys. Rev. A* **2005**, *71*, 013423.
- [28] Trallero-Herrero, C.; Cohen, J.L.; Weinacht, T. *Phys. Rev. Lett.* **2006**, *96*, 063603.
- [29] Trallero-Herrero, C.; Weinacht, T.C. *Phys. Rev. A* **2007**, *75*, 063401.
- [30] Chuntunov, L.; Rybak, L.; Gandman, A.; Amitay, Z. *Phys. Rev. A* **2008**, *77*, 021403.
- [31] Chuntunov, L.; Rybak, L.; Gandman, A.; Amitay, Z. *J. Phys. B* **2008**, *41*, 035504.
- [32] Amitay, Z.; Gandman, A.; Chuntunov, L.; Rybak, L. *Phys. Rev. Lett.* **2008**, *100*, 193002.

- [33] Chuntanov, L.; Rybak, L.; Gandman, A.; Amitay, Z. *Phys. Rev. A* **2010**, *81*, 045401.
- [34] Eitan, R.; Mundt, M.; Tannor, D.J. *Phys. Rev. A* **2011**, *83*, 053426.
- [35] Palao, J.P.; Reich, D.M.; Koch, C.P.; NIST ASD Team. *Phys. Rev. A*, submitted for publication, 2013.

Appendix 1. Method of degenerate kernels for the numerical solution of Fredholm equations of the second kind

To simplify notation, we map the time interval from $[0, T]$ to $[0, 1]$. A degenerate kernel is obtained by a tensor product ansatz for the true kernel,

$$\mathcal{K}(t, t') \simeq \sum_{j,k=0}^N d_{jk} \alpha_j(t) \beta_k(t'),$$

with $\delta_j(t') = \sum_{k=0}^N d_{jk} \beta_k(t')$, taking the basis functions to be [21,22]

$$\alpha_j(t) = \beta_j(t) = \begin{cases} 1 - N \left| t - \frac{j}{N} \right|, & \frac{j-1}{N} \leq t \leq \frac{j+1}{N}, \\ 0, & \text{else.} \end{cases} \tag{12}$$

N is the order of the approximation. At the grid points $t = u/N$, $t' = v/N$,

$$\mathcal{K}_N \left(\frac{u}{N}, \frac{v}{N} \right) = \sum_{j,k=0}^N d_{jk} \delta_{ju} \delta_{kv}.$$

The choice of basis functions suggests for the coefficients

$$d_{jk} = \mathcal{K}_N \left(\frac{j}{N}, \frac{k}{N} \right) = \mathcal{K}_N(t_j, t_k),$$

such that \mathcal{K}_N reasonably approximates $\mathcal{K}(t, t')$ on a time grid of size $N + 1$.

It can be shown that the solution to Equation (10) is given by Equation (11) with X_j the solution of the following system of linear equations,

$$[\mathbb{1}_{N+1} - \gamma \mathbf{C}] \mathbf{X} = \gamma \mathbf{b}, \tag{13}$$

with matrix elements

$$C_{jk} = \sum_{i=0}^n K(t_j, t_i) \int_0^1 \alpha_i(t) \alpha_k(t) dt \equiv \sum_{i=0}^n K(t_j, t_i) A_{ik},$$

where

$$A_{ik} = \int_0^1 \alpha_i(t) \alpha_k(t) dt = \begin{cases} \frac{1}{3n}, & \text{for } i = k = 0 \text{ or } i = k = n \\ \frac{2}{3n}, & \text{for } i = k, 1 \leq i \leq n \\ \frac{1}{6n}, & \text{for } i = k + 1 \text{ or } i = k - 1 \\ 0, & \text{else} \end{cases}$$

and

$$b_k = \int_0^1 I(t) \left[\sum_{i=0}^n K(t_k, t_i) \alpha_i(t) \right] dt.$$